SUPPORTING INFORMATION

Emergence of Magnetic Monopole-like Behavior in Iron Oxide Nanoparticles Grafted with Chiral Brushes: A Chiral Induced Spin Selectivity Manifestation

Elizabeth Shiby,[1,#] Yu Shao,[2,3,#] Minh Dang Nguyen,[4,#] Puja Thapa,[5] Supriya Ghosh,[1] Ishwari Chaitanya Joshi,[2] Yuming Huang,[2] Supawitch Hoijang,[4] Ramtin Yarinia,[4] Christopher K. Ober,[2] T. Randall Lee,[4] Dali Sun,[5] Brian P. Bloom,[1]* and David H. Waldeck[1,†]

[1]*Department of Chemistry, University of Pittsburgh, Pittsburgh, Pennsylvania 15260, United States*
[2]*Department of Materials Science and Engineering, Cornell University, Ithaca, New York 14853, United States*
[3]*Chemical and Biomolecular Engineering, University of Notre Dame, South Bend, Indiana, 46637, United States*
[4]*Department of Chemistry and the Texas Center for Superconductivity, University of Houston, Houston, Texas 77204, United States*
[5] *Department of Physics, North Carolina State University, Raleigh, North Carolina, 27695, United States*
[#]These authors contributed equally to this work.
[†] Deceased

*Correspondence: bpb8@pitt.edu

EXPERIMENTAL SESSION

METHODS

Materials. Iron(III) acetylacetonate ($Fe(acac)_3$) (99.9%, Sigma–Aldrich), 4-biphenylcarboxylic acid (BPC) oleic acid (OA) (90%, Sigma–Aldrich), and benzyl ether (98%, Sigma–Aldrich) were used for synthesis of 23 nm Fe_3O_4 nanocubes. Iron(III) chloride hexahydrate ($FeCl_3 \cdot 6H_2O$) (97%, Alfa Aesar), ethylene glycol (EG) (99%, Sigma–Aldrich), diethylene glycol (EDG) (99%, Thermo Scientific), sodium acetate (NaAc) (99%, anhydrous, ACROS Organic), sodium acrylate (97%, Sigma–Aldrich), polyethylene glycol (PEG-400) (average M_n 400, Sigma–Aldrich) were used for synthesis of 203 nm Fe_3O_4 nanospheres. Igepal CO-520 (average M_n 441, Sigma–Aldrich), cyclohexane (Oakwood), tetraethyl orthosilicate (TEOS) (99%, Sigma–Aldrich), ammonia solution (NH_4OH) (28–30%, VWR Chemicals), 3-aminopropylethoxy silane (APTES) (Oakwood), and ethanol (200 Proof, Decon Labs) were used for silica coating and amino functionalization. *L*-phenylalanine (≥98%, Sigma–Aldrich), *D*-phenylalanine (≥98%, Sigma–Aldrich) triphosgene (98%, Sigma–Aldrich), (±)-propylene oxide (99%, Sigma–Aldrich), tetrahydrofuran (THF) (≥99.9%, anhydrous, inhibitor-free, Sigma–Aldrich), *N*,*N*-dimethylformamide (DMF) (≥99.8%, anhydrous, Sigma–Aldrich), chloroform (≥98%, Macron Fine Chemicals), acetone (≥99.5%, Macron Fine Chemical). All chemicals were used for synthesis without any further purification. Deionized (DI) water with resistance of 18 MΩ-cm (Academic Milli-Q Water System, Millipore Corporation).

Synthesis of Fe_3O_4 Nanoparticles. In this study, two types of Fe_3O_4 NPs were synthesized: 23 nm ferrimagnetic single-domain Fe_3O_4 nanocubes and 203 nm superparamagnetic multidomain Fe_3O_4 nanospheres. These NPs were prepared via thermal decomposition and solvothermal methods, respectively, as reported by Nguyen and co-workers.[1] The synthesis procedures are briefly described below:

Synthesis of 23 nm Ferrimagnetic Single-Domain Fe_3O_4 Nanocubes- 0.7 g of $Fe(acac)_3$ and 0.4 g of BPC were mixed with 1.13 g of OA and 15 mL of benzyl ether. Prior to heating, the mixture was degassed under a nitrogen atmosphere for 1 h. The reaction mixture was then heated to 293 °C at a rate of ~39 °C/min and left for 30 min. After cooling to room temperature, the product was collected and washed with ethanol by centrifugation. The resulting NPs were dried for 4–6 h and stored in a vacuum desiccator for subsequent silica coating.

Synthesis of 203 nm Superparamagnetic Multidomain Fe_3O_4 Nanospheres- 2.7 g of $FeCl_3 \cdot 6H_2O$ was dissolved in 40 mL of an EG/DEG mixture (15 mL of EG and 25 mL of DEG). Then, 7.2 g of NaAc was added to the solution, followed by the addition of another 40 mL of the EG/DEG mixture. The mixture was magnetically stirred for 30 min. Subsequently, 2.4 mL of PEG-400 was injected, and the reaction was heated to 188 °C and maintained at that temperature for 5 h. After cooling to room temperature, the product was collected and washed several times with ethanol by magnetic separation. The resulting NPs were then redispersed in ethanol for subsequent silica coating.

Silica Coating of Fe_3O_4 (Fe_3O_4@SiO_2) Nanoparticles. To prevent oxidation of the obtained magnetic NPs and facilitate subsequent surface modification, the NPs were encapsulated within a silica shell. Two different silica coating approaches were employed: the reverse micelle method[2] for the 23 nm Fe_3O_4 nanocubes and the Stöber method[3-4]for the 203 nm Fe_3O_4 nanospheres. Each method is briefly provided below:

Silica Coating of 23 nm Ferrimagnetic Single-Domain Fe_3O_4 Nanocubes. 0.5 g Igepal CO-520 surfactant was mixed with 11 mL cyclohexane. While the mixture was vigorously stirred, 4.4 mL of 2.5 mg/mL dispersion of Fe_3O_4 nanocubes in cyclohexane was added. After magnetic stirring for 10 min, 100 mL of NH_4OH was added dropwise, followed by stirring for another 10 min. Then, 75 mL of TEOS was rapidly added, and the reaction mixture was stirred at room temperature overnight. The resulting product was collected and washed several times with ethanol by centrifugation. The final NPs were dried overnight for subsequent surface functionalization.

Silica Coating of 203 nm Superparamagnetic Multidomain Fe_3O_4 Nanospheres. 2.5 mL of the obtained Fe_3O_4 dispersion was mixed with 77.5 mL of ethanol and 20 mL of DI water. The mixture was placed in a sonication bath for 1.5 h, followed by mechanical stirring for 10 min. Then, 2.4 mL of NH_4OH was rapidly added, and the mixture was stirred for another 10 min. Subsequently, 183 mL of TEOS was added dropwise and stirred at room temperature overnight. The product was collected and washed several times with ethanol by magnetic separation. The final NPs were then dried overnight for subsequent surface functionalization.

Amine-Functionalization of Fe_3O_4@SiO_2 Nanoparticles. To enable further growth with chiral polymers, the surfaces of the obtained Fe_3O_4@SiO_2 NPs were functionalized with amine ($–NH_2$) groups using APTES as a surface modifier. This approach was adapted from previously reported studies.[5] [6]In a typical procedure, 0.1 g of dried Fe_3O_4 powder was dispersed in 80 mL of ethanol. The dispersion was sonicated for 1 h, followed by mechanical stirring for 10 min. While stirring, 4.8 mL of NH_4OH was rapidly added, and the mixture was stirred for an additional 10 min. Subsequently, 0.25 mL of APTES was added, and the mixture was stirred at room temperature overnight, then refluxed at 88 °C for 1 h. After cooling to room temperature, the product was collected and washed several times with ethanol. The final NPs were dried overnight for subsequent growth with chiral polymers.

Synthesis of N-carboxyanhydrides (NCA) Monomer. NCA monomers were synthesized using previously reported protocol.[7] Briefly, to a pressure vessel with a heavy wall, 1.0 g of *L*- or *D*-phenylalanine (*L*- or *D*-Phe) (6.1 mmol, 1.0 eq), 15 mL of THF, and 4.3 mL of propylene oxide (60 mmol, 10.0 eq) were added sequentially under magnetic stirring. Then, 897 mg of triphosgene (4.0 mmol, 0.5 eq) was added in one portion, and the vessel was immediately sealed. The reaction mixture was stirred at room temperature for 7 h and then cooled down to ~4 °C in an ice bath. For safety, excess triphosgene was quenched by the addition of 10 mL cold water (~4 °C) with stirring for 1–3 min. The mixture was extracted twice with ethyl acetate (2×20 mL) at room temperature. The combined organic layers were washed with brine and dried over anhydrous Na_2SO_4. After solvent removal by rotatory evaporation under vacuum at 45 °C, the crude product was purified by recrystallization twice in a hexane/ethyl acetate mixture at 4 °C. The purified product was obtained as white needle-like crystals (961 mg, yield = 83%) and stored at -20 °C up to 1 month.

Synthesis of Poly(L-Phe)- and Poly(D-Phe)-Decorated Fe_3O_4 Nanoparticles. Two types of amine-functionalized Fe_3O_4@SiO_2 NPs—featuring either 23 nm nanocube or 203 nm nanosphere Fe_3O_4 cores—were grafted with chiral polymers, poly(*L*-Phe) or poly(*D*-Phe), via surface-initiated ring-opening polymerization of NCA monomers, following a previously reported protocol.[8] In a typical synthesis, 20 mg of amine-functionalized Fe_3O_4@SiO_2 powder was dispersed in 2 mL of anhydrous DMF in a Schlenk flask. The dispersion was sonicated for 20 min, followed by the addition of a small magnetic stir bar and stirred at 1000 rpm. Then, 30–80 mg of NCA monomers dissolved in 2 mL of anhydrous ethyl acetate was slowly injected into the flask. The reaction mixture was mechanically stirred at 1000 rpm for 24–48 h under a nitrogen atmosphere. The resulting composite NPs were collected by magnetic separation and sequentially washed 5 times with ethanol, chloroform, and acetone to remove unreacted polymers and crosslinked aggregates. The final NPs were dried and used for further characterization by several techniques, such as NMR, CD, FT-IR, TGA, and TEM.

2.2 CHARACTERIZATION

Material Characterization. Sample morphology was analyzed using a transmission electron microscope (TEM, JEOL JEM-2010) operated at an accelerating voltage of 200 kV and a scanning electron microscope (SEM, JSM-6330F) operated at 15 kV. TEM samples were prepared by drop-casting onto 300-mesh holey carbon-coated copper grids. Phase composition was determined using X-ray diffractometer (XRD, Smart Lab, Rigaku) with Cu Kα irradiation, operated at 40 kV and 44 mA, with a step of 0.02°. XRD samples were drop-casted onto clean glass slides. Surface functionality was characterized by X-ray photoelectron spectroscopy (XPS, PHI 5700) using a monochromatic Al Kα X-ray source. The adventitious carbon C 1s peak at 284.8 eV was used for referencing the binding energy of the spectra. For XPS and SEM measurements, samples were drop-casted onto clean silicon wafers.

AFM and MFM Measurements. Samples were prepared by sonicating a 0.001 mg/mL chloroform solution of the chiral polymer-grafted NPs for ~5 min, followed by drop-casting 20 µL onto a gold-coated silica substrate. After allowing the chloroform to evaporate, the samples were used for measurements. The AFM measurements were performed on a Bruker icon VI instrument using a Co/Cr tip with a force constant of 2.8 N/m. MFM is a type of AFM measurement that uses a magnetized tip to detect magnetic interactions between the tip and the material—in this case, a nanoparticle. The operation is performed in a two-pass lift mode: in the first pass, the sample's topography is recorded, and in the second pass, the tip is lifted to a fixed height above the surface, where long-range magnetic interactions dominate over short-range van der Waals forces.[9,11] These magnetic interactions can be either attractive or repulsive, thereby affecting the cantilever's phase signal. Prior to the MFM measurements, AFM tips were magnetized from the bottom using a permanent magnet for ~5 mins. The topography was measured in the non-contact mode in the first pass, and then in the second pass, the MFM was measured after lifting to a height of 125 nm. The phase change was calculated from the MFM image by drawing a line profile through the center of the nanoparticle. The maximum height of the peak with respect to the gold reference was used to calculate g_{φ}.

Magnetometry. All the magnetic properties were measured using a Quantum Design MPMS3 SQUID magnetometer. The magnetic moment for single-domain and multidomain samples were measured in the temperature range from 2.5-300 K and field range up to 7 T. For the M-H loop, we have applied the magnetic field from 7T to 7T while keeping the temperature constant. The M-T curve was measured at a constant applied magnetic field under zero-field-cooled (ZFC) and field-cooled (FC) condition, respectively.

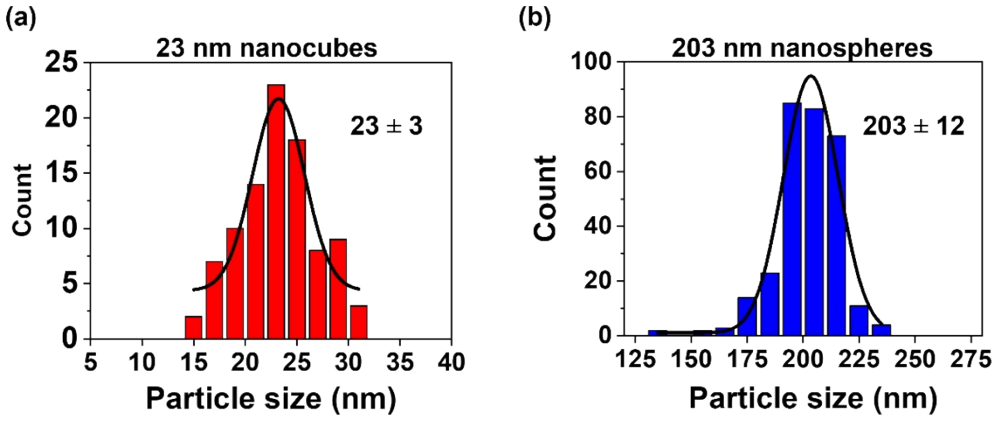

Figure S1. Size distribution of (a) 23 nm FiM single-domain and (b) 203 nm SPM multidomain Fe_3O_4 NPs. Note that the sizes in (a) and (b) refer to the edge length measured from TEM images and the diameter measured from SEM images, respectively.

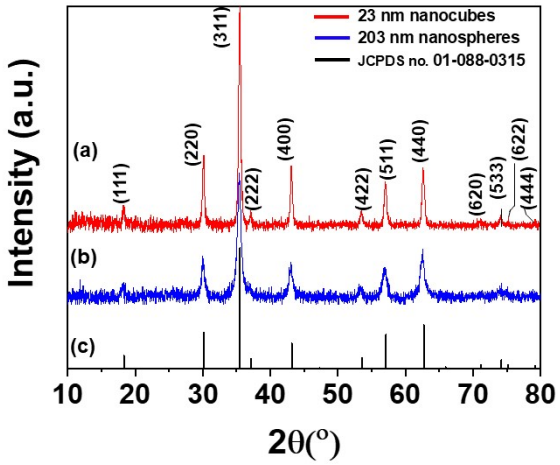

Figure S2. XRD patterns of (a) 23 nm FiM single-domain nanocubes and (b) 203 nm SPM multidomain Fe_3O_4 nanospheres (c) reference lines of Fe_3O_4 phase (JCPDS no. 01-088-0315).

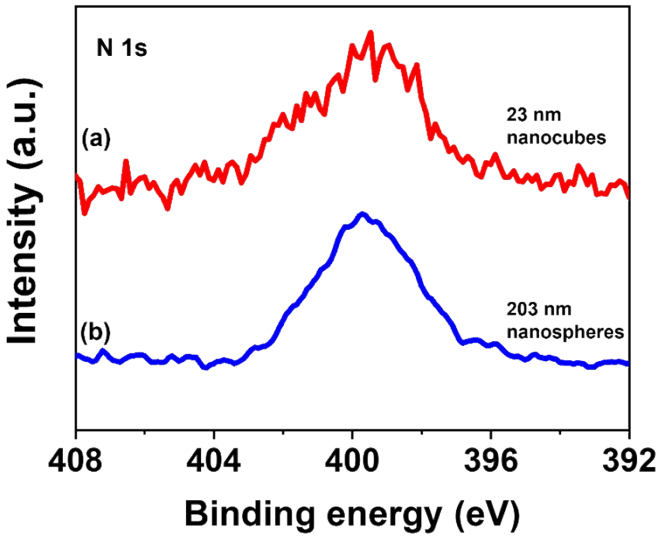

Figure S3. High-resolution N 1s XPS spectra of APTES-functionalized Fe_3O_4 NPs of (a) 23 nm FiM single-domain nanocubes and (b) 203 nm SPM multidomain nanospheres.

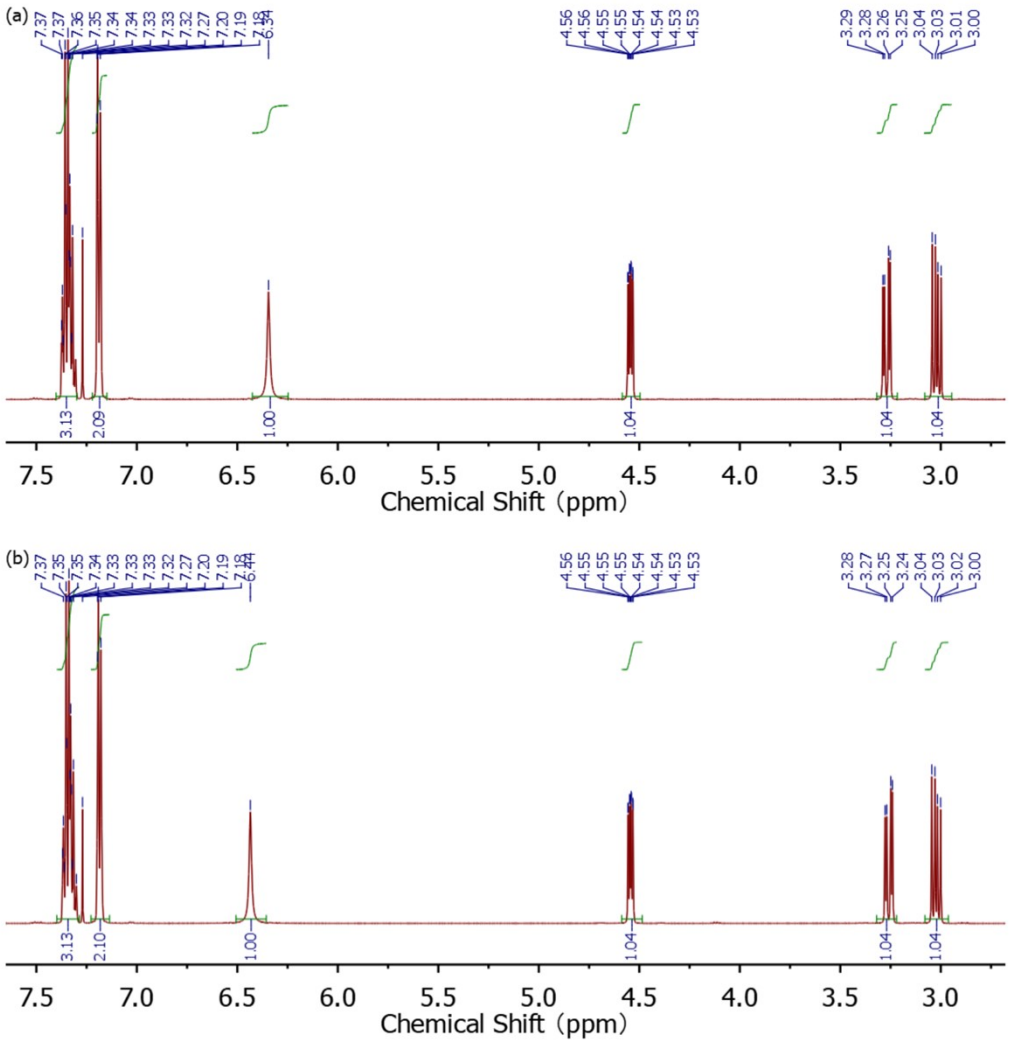

Figure S4. ^{1}H NMR spectra of (a) *D*- and (b) *L*-phenylalanine NCA monomers.

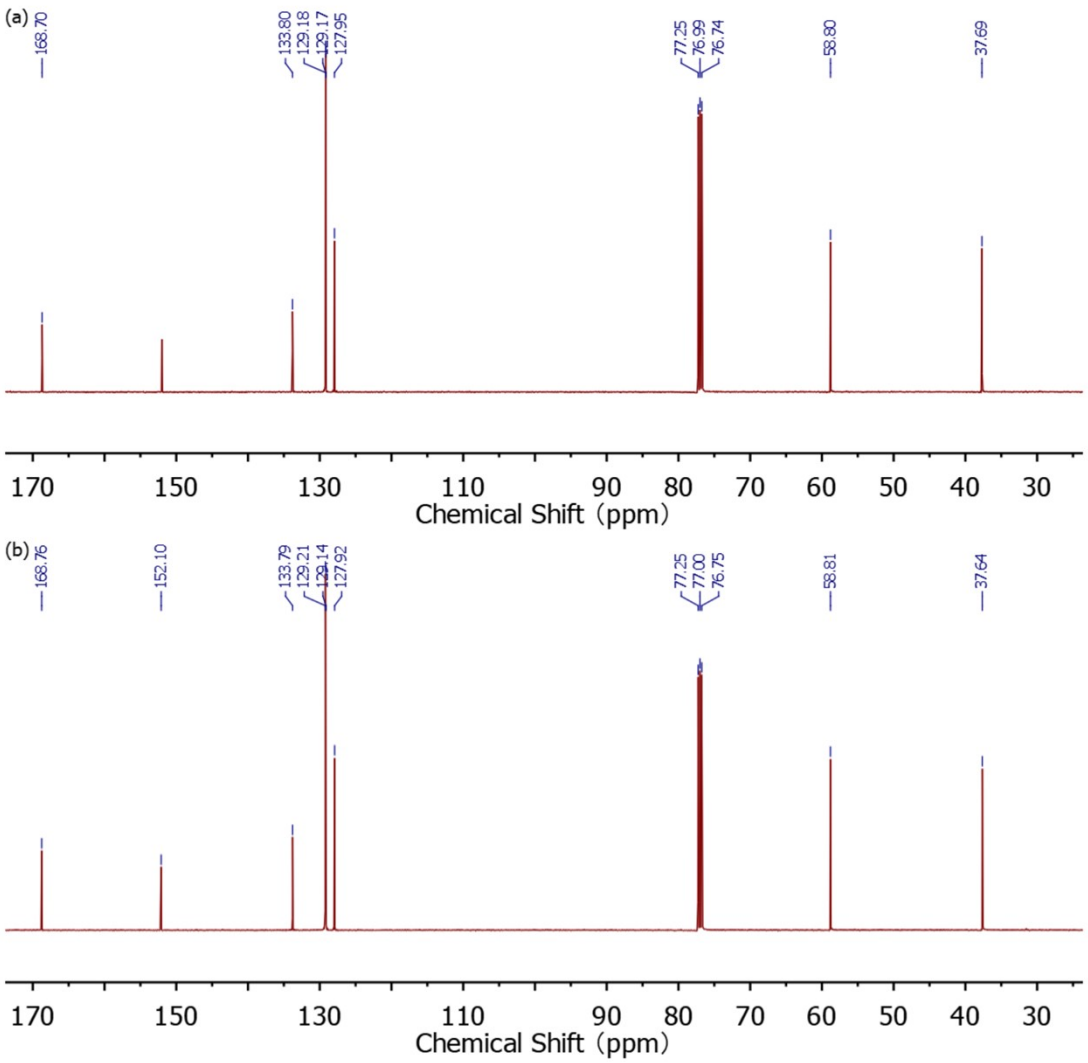

Figure S5.[13]C NMR spectra of (a) *D*- and (b) *L*-phenylalanine NCA monomers.

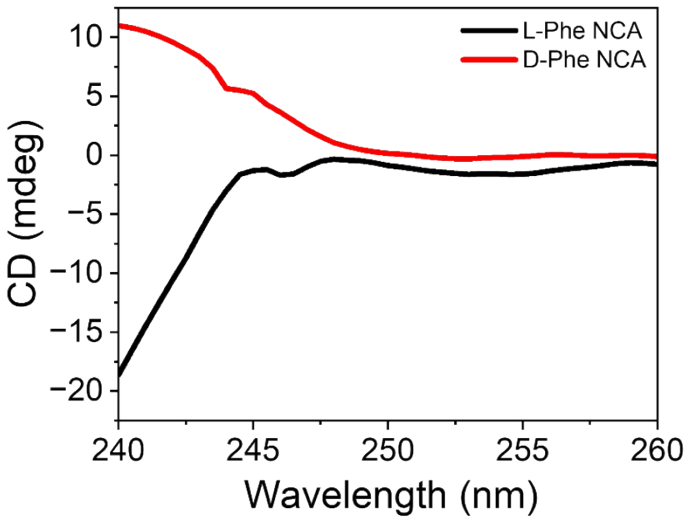

Figure S6. Circular Dichroism (CD) spectra of L- and *D*-phenylalanine NCA polymers grafted on the 203 nm SPM multidomain Fe_3O_4 nanospheres.

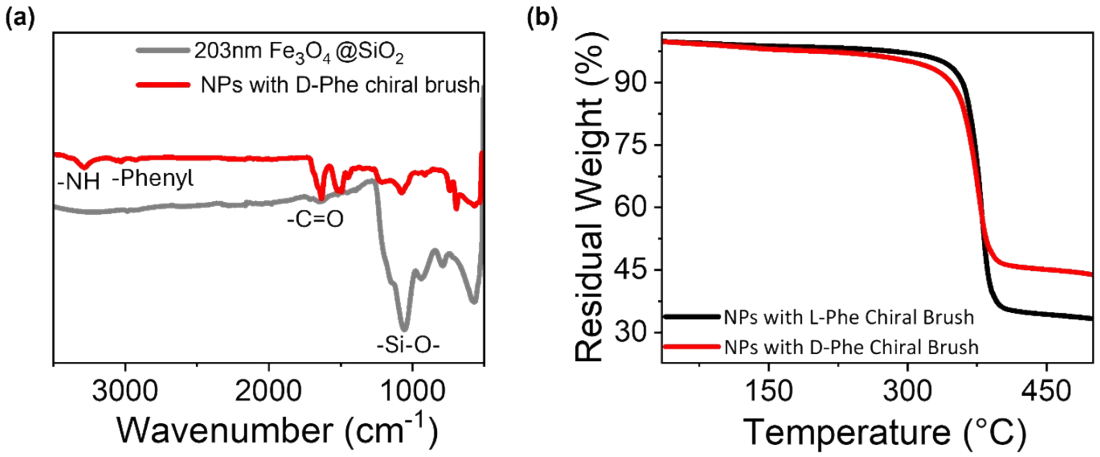

Figure S7.a) Representative FT-IR spectra of SPM multidomain NPs before and after the grafting of D-Phe chiral brushes. b) Thermogravimetric analysis curve for polymer-grafted 203 nm SPM multidomain Fe_3O_4 nanospheres.

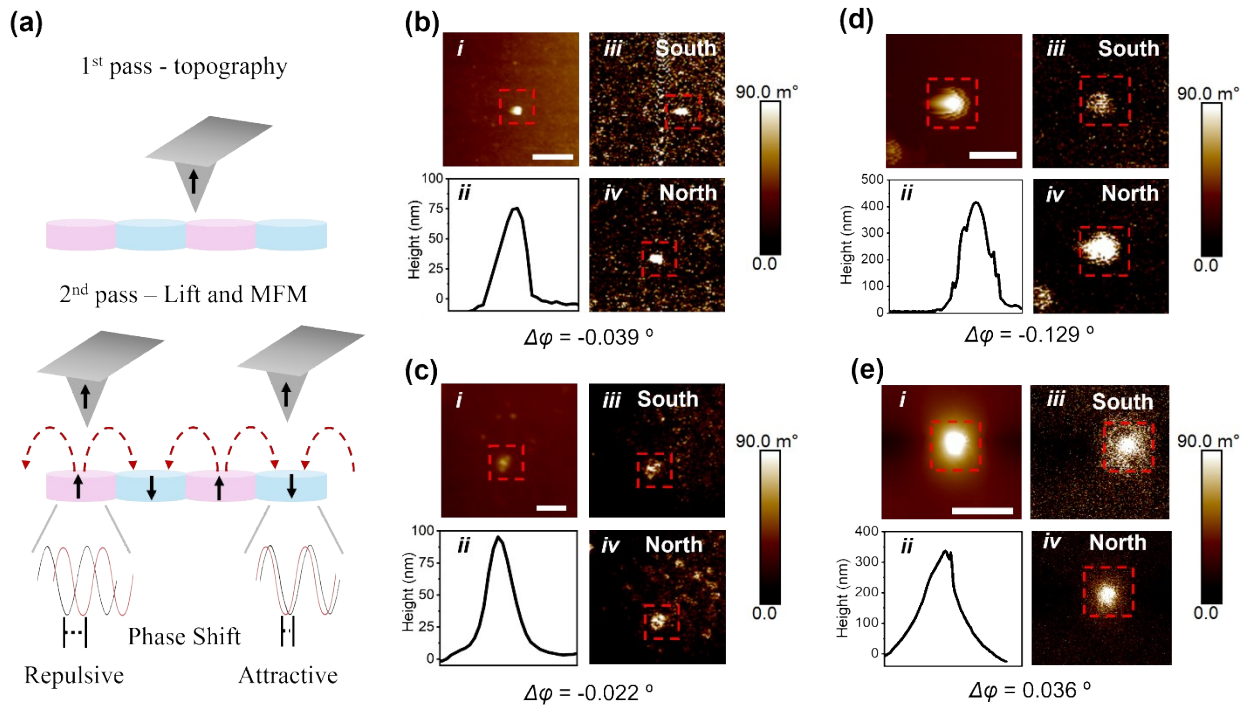

Figure S8. (a) Schematic representation of the MFM technique. (b–e) AFM topography (*i*) and height profile (*ii*) of an additional set of NPs. Corresponding MFM images with a South (*iii*) and North (*iv*) magnetized tip are shown in each panel. Panel (b) shows *L*- and panel (c) shows *D*-Phe-coated 23 nm FiM single-domain Fe_3O_4 nanocubes. Panel (d) shows *L*- and panel (e) shows *D*-Phe-coated 203 nm SPM multidomain Fe_3O_4 nanospheres. The red square indicates the measured nanoparticle and the change in phase, $\Delta\varphi$, is reported beneath each panel. The scale bar corresponds to 2 µm.

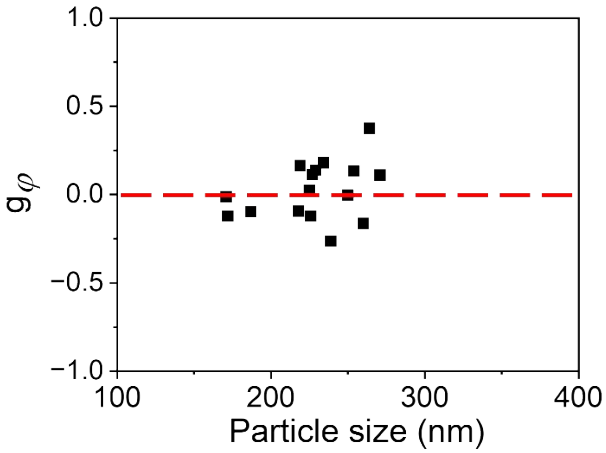

Figure S9. Correlation between asymmetry in phase shift, g_φ, with the radius of SPM multidomain Fe_3O_4 NPs without chiral brushes.

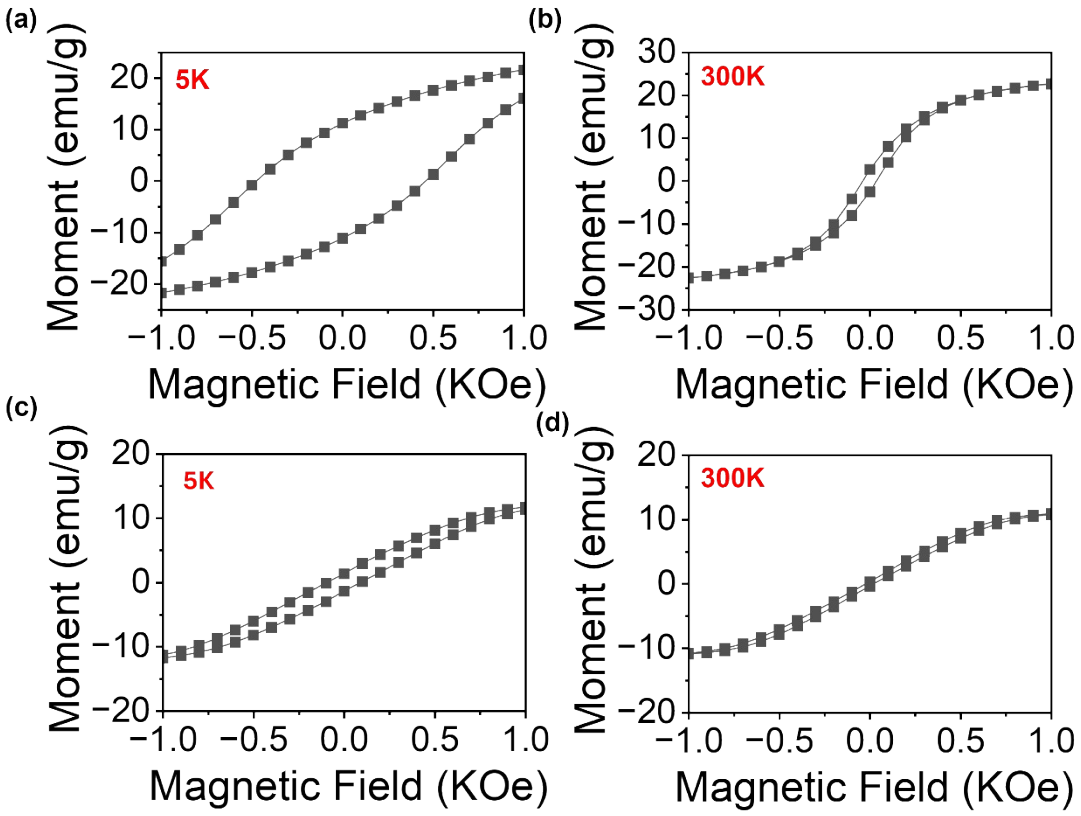

Figure S10:M-H curves collected at a) 5 K and b) 300 K for 23 nm FiM single-domain nanocubes, and at c) 5 K and d) 300 K for 203 nm SPM multidomain Fe_3O_4 nanospheres.

References

[1] Nguyen, M. D.; Deng, L.; Lee, J. M.; Resendez, K. M.; Fuller, M.; Hoijang, S.; Robles-Hernandez, F.; Chu, C.-W.; Litvinov, D.; Hadjiev, V. G.; Xu, S.; Phan, M.-H.; Lee, T. R. Magnetic Tunability via Control of Crystallinity and Size in Polycrystalline Iron Oxide Nanoparticles. *Small* 2024, **20**, 2402940.

[2]Ding, H. L.; Zhang, Y. X.; Wang, S.; Xu, J. M.; Xu, S. C.; Li, G. H. Fe_3O_4@SiO_2 Core/Shell Nanoparticles: The Silica Coating Regulations with a Single Core for Different Core Sizes and Shell Thicknesses. *Chem. Mater.* 2012, **24**, 4572–4580.

[3]Stober, W.; Fink, A.; Bohn, E. J. Controlled Growth of Monodisperse Silica Spheres in the Micron Size Range. *J. Colloid Interface Sci.* 1968, **26**, 62–69.

[4]Chi, Y.; Yuan, Q.; Li, Y.; Tu, J.; Zhao, L.; Li, N.; Li, X. Synthesis of Fe_3O_4@SiO_2–Ag Magnetic Nanocomposite Based on Small-Sized and Highly Dispersed Silver Nanoparticles for Catalytic Reduction of 4-Nitrophenol. *J. Colloid Interface Sci.* 2012, **383**, 96–102.

[5]Hoijang, S.; Wangkarn, S.; Ieamviteevanich, P.; Pinitsoontorn,S.; Ananta, S.; Lee, T. R.; Srisombat, L. Silica-Coated Magnesium Ferrite Nanoadsorbent for Selective Removal of Methylene Blue. *Colloids Surf., A: Physicochem. Eng. Asp.* 2020, **606**, 125483.

[6] Kim, J.-H.; Chung, H.-W.; Lee, T. R. Preparation and Characterization of Palladium Shells with Gold and Silica Cores. *Chem. Mater.* 2006, **18**, 4115–4120.

[7] Hoijang, S.; Kunakham, T.; Nonkumwong, J.; Faungnawakij, K.; Ananta, S.; Nimmanpipug, P.; Lee, T. R.; Srisombat, L. Surface Modification of Magnesium Ferrite Nanoparticles for Selective and Sustainable Remediation of Congo Red. *ACS Appl. Nano Mater.* 2021, **4**, 10244–10256.

[8]Tian, Z.-Y.; Zhang, Z.; Wang, S.; Lu, H. A Moisture-Tolerant Route to Unprotected α/β-Amino Acid *N*-Carboxyanhydrides and Facile Synthesis of Hyperbranched Polypeptides. *Nat Commun*. 2021, **12**, 5810.

[9]Liu, D.; Li, Y.; Deng, J.; Yang, W. Synthesis and Characterization of Magnetic Fe_3O_4-Silica-Poly(γ-benzyl-*L*-glutamate) Composite Microspheres. *Reac. Funct. Polym.* 2011, **71**, 1040–1044.

[10] Passeri, D.; Dong, C.; Reggente. M.; Angeloni, L.; Barteri, M.; Scaramuzzo, F. A.; De Angelis, F.; Marinelli, F.; Antonelli, F.; Rinaldi, F.; Marianecci, C.; Carafa, M.; Sorbo, A.; Sordi, D.; Arends, I. W.; Rossi, M. Magnetic Force Microscopy: Quantitative Issues in Biomaterials. *Biomatter* 2014, **4**, e29507.

[11] Schreiber, S.; Savla, M.; Pelekhov, D. V.; Iscru, D. F.; Selcu, C.; Hammel, P. C.; Agarwal, G. Magnetic Force Microscopy of Superparamagnetic Nanoparticles. *Small* 2008, **4**, 270–278.